

Progress in SOL and Divertor Studies on the MAST Tokamak

J-W. Ahn^a, G.F. Counsell, A.Kirk, A.Tabasso, P.Helander, Y.Yang^b

Euratom/UKAEA Fusion Association, Culham Science Centre, Abingdon, Oxon OX14 3DB, UK

^a*Department of Physics, Imperial College of Science, Technology and Medicine, London SW7 2BZ, UK*

^b*Institute of Plasma Physics, Hefei, 230031, P.R.China*

1. Introduction

Understanding the physical processes governing the transport of heat and particles to the divertor targets, and developing methods for mitigating their impact, are of particular importance for the spherical tokamak (ST), where the geometry leads to significantly smaller wetted areas than in conventional devices, particularly on the inboard side. Recent improvements to the NBI heating and gas fuelling systems have broadened the operational space of MAST and various new and enhanced diagnostics have allowed measurements of a wealth of boundary plasma data.

The plasma performance so far includes up to 1.2 MA of plasma current, significant NBI heating with powers in excess of $P_{NBI} \sim 2.5$ MW from two beam lines and routine access to H-mode both in Ohmic and NBI heated plasmas. MAST typically has an asymmetric double-null divertor configuration, for which the degree of magnetic asymmetry is characterised by the separation, δr_{sep} , of the inner and outer separatrices at the mid-plane. A total of 192 Langmuir probes in 10 arrays are used as a main diagnostic tool to measure edge plasma parameters with a time resolution of around 1ms. The probes are spaced 3mm apart at the inboard side and 10mm at the outboard. D_α and D_γ light emission is simultaneously resolved by a photo multiplier and a spectrometer. Edge D_α emission at the midplane is collected with a linear camera. The outboard midplane SOL is accessed by a fast reciprocating probe (RP).

2. SOL scaling and characterisation

2.1 Scaling for the MAST SOL width

The mid-plane heat flux scrape-off layer (SOL) width, Δ_h , plays a key role in determining divertor power loadings. MAST explores extreme parameter regimes such as ρ_i/Δ_h , ρ_i the ion Larmor radius, which is ~ 1 but $\ll 1$ in conventional devices. A scaling law for the SOL width

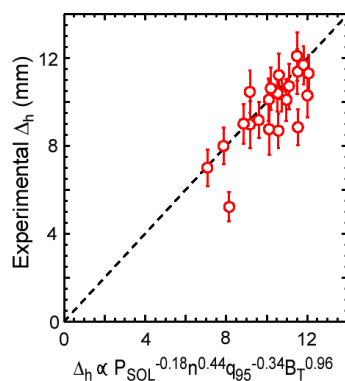


Fig.1 Midplane SOL width scaling in sheath-limited regime

in MAST for the sheath-limited regime has been developed by flux mapping data from the target Langmuir probe arrays to the midplane and fitting to key engineering parameters, indicating a weak negative dependence with power flow across the SOL, P_{SOL} , (e.g. $\Delta_h \propto P_{SOL}^{-0.18} n_e^{0.44} q_{95}^{-0.34} B_{t,mag}^{0.96}$ for the outboard SOL in sheath-limited L-mode, see Fig.1). Scalings for the conduction-limited SOL and comparison with results from conventional device are underway.

2.2 Onion-skin modelling

SOL width scalings are being complemented by advanced Onion-skin Modelling (OSM2), from which upstream data are

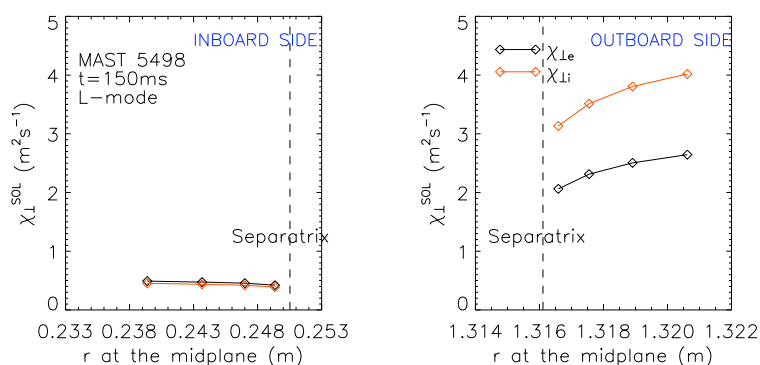


Fig.2 χ_{\perp}^{SOL} values for inboard and outboard sides calculated from the upstream and target parameter values using a simple SOL model

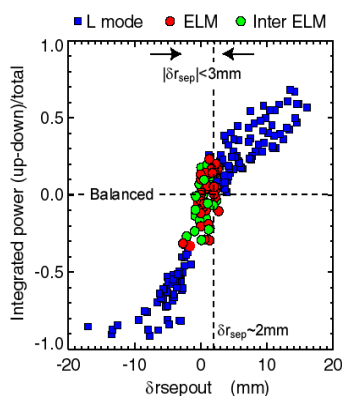
low aspect ratio in the ST appears as an effective particle and momentum source term and drives strong upstream flows at a significant fraction of the Mach number, M . Outboard mid-plane reciprocating probe measurements seemed to confirm the existence of upstream flows with $M \sim 2$, comparable to OSM2 predictions.

3. Power accounting and balance

The j_{sat}^+ and T_e values measured by Langmuir probes are used to evaluate the heat flux density arriving at target probes, $q = \gamma k T_e j_{sat}^+ / e$, taking a sheath heat transmission coefficient $\gamma = 7$. The total power flowing to each target is obtained by toroidally integrating exponential fits to the data over strike points.

3.1 Outer/inner power balance

The outer/inner power ratio, R_{oi} , exceeded 25:1 for L-mode plasmas and at ELM peaks but fell to around 10:1 during inter-ELM periods (see Fig.3). In lower ELM frequency (therefore longer inter-ELM periods) discharges R_{oi} falls even further, to around 4:1, comparable with the ratio of surface areas for the outboard and inboard separatrices. During L-mode and at ELM peaks, the transport is enhanced by poloidally asymmetric processes more prominent on the low field, bad curvature outboard side.



3.2 Up/down power balance

Ion $B \times \nabla B$ drift (currently towards the lower X-point) effect seems to play a role in up/down power balance. The ratio of power to the lower targets compared to the upper, R_{lu} , was ~ 1.5 for magnetically symmetric plasmas ($\delta r_{sep} \sim 0$, CDN) and reached unity, balanced power between the

Fig.4 Ratio of integrated power flowing between upper and lower sides as a function of δr_{sep}

produced to extract perpendicular heat and particle diffusion coefficients, χ_{\perp}^{SOL} and D_{\perp}^{SOL} , using a simple SOL model (see Fig.2). χ_{\perp}^{SOL} is significantly higher on the outboard side with values of 6~7 times those on the inboard side and shows a Bohm-like χ_{\perp} behaviour, $\propto T/B$. It also revealed [1] that the particularly large mirror force ($\propto \nabla B/B$) due to the

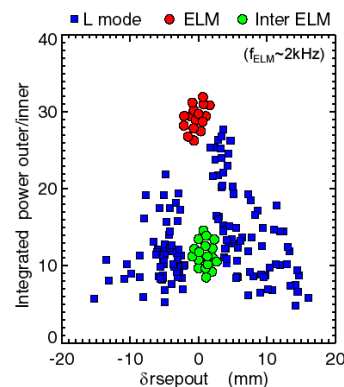


Fig.3 Ratio of integrated power flowing between outer and inner sides as a function of δr_{sep}

upper and lower targets, for $\delta r_{sep} \sim 2\text{mm}$. Only L-mode regimes were encountered for large values of δr_{sep} (quasi-SND plasmas) but H-mode access was achieved for CDN configurations, with $\delta r_{sep} < \sim 3\text{mm}$ (see Fig.4). [2]

4. ELM characteristics

ELMs in MAST feature characteristics of type-III ELMs in conventional tokamaks; the ELM frequency, f_{ELM} , falls with increasing P_{SOL} and rises with increasing \bar{n}_e .

4.1 At the target

ELMy H-modes were only observed to occur in CDN configuration discharges and the bulk (> 94%) of energy released during ELMs flows to the outboard side. The outboard strike-points shift radially outward during ELMs by up to $\sim 3\text{cm}$. Virtually no SOL width broadening, however, has been observed during the ELM. The peak heat fluxes rise by < factor 2 at the inboard but > factor 4 at the outboard (reaching $\sim 4\text{MW/m}^2$ for $P_{NBI} \sim 2\text{MW}$). [2]

4.2 At the mid-plane

The ion saturation current, j_{sat}^+ , measured by the mid-plane RP is as large as values observed at the outboard targets during ELM peaks. The magnitude of j_{sat}^+ bursts to the RP probe are rather variable, even for similar size ELMs at the targets. The RP typically measures ELM periods of less than $50\mu\text{s}$ compared to $\sim 300\mu\text{s}$ at the target, which allows one to resolve ‘multiple’ ELMs at the target into discrete bursts. The j_{sat}^+ bursts are shifted in time with respect to the peak of D_α emission at the targets and the delays appear to be consistent with a radial motion of the bursts at a velocity of around 1.5km/s . [3]

5. Divertor detachment

Reduction of target power loads by radiative detachment is being explored. The roll-over and then decrease of the ion flux and temperature with the increase of core line averaged density has been achieved in MAST at both the inboard and outboard targets, for Ohmic and L-mode plasmas. In H-mode the plasma is in a partially detached state during inter-ELM periods and re-attaches during ELMs. Detachment starts to occur at \bar{n}_e of $3.5 \times 10^{19} \text{ m}^{-3}$ for both the inboard and outboard targets. The degree of detachment of the inboard targets is estimated as $\text{DOD} \sim 20$ at $\bar{n}_e \sim 6.5 \times 10^{19} \text{ m}^{-3}$, which was calculated from a parabolic fit to j_{sat}^+ in the conduction-limited regime at densities below $\bar{n}_e \sim 3.5 \times 10^{19} \text{ m}^{-3}$ (see Fig.5). The DOD was lower at the outboard targets for the same density, $\text{DOD} \sim 6$, as observed on conventional devices.

MAST can operate at a density well above the Greenwald limit and that is probably why detachment could be achieved despite the fully open nature of the MAST divertor and the

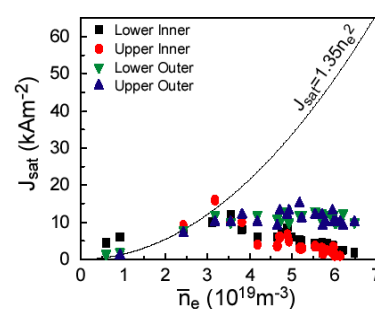


Fig.5 Target plasma detachment with j_{sat}^+ roll-over starting at $\bar{n}_e \sim 3.5 \times 10^{19} \text{ m}^{-3}$. The solid line overlaid represents the extrapolated ion fluxes to the quadratic law

horizontal nature of the outboard targets. Target plasma densities at roll-over are substantially lower than has been reported in other tokamaks, $n_t \sim 2 \times 10^{18} \text{ m}^{-3}$. [4]

6. Biased divertor operations

Convective cells driven by a toroidally varying negative bias of the divertor plates have been theoretically predicted [5] to show up to a factor 4 broadening of the heat flux SOL width at the target, indicating that this method might be able to be used to diminish target plate erosion in addition to divertor detachment.

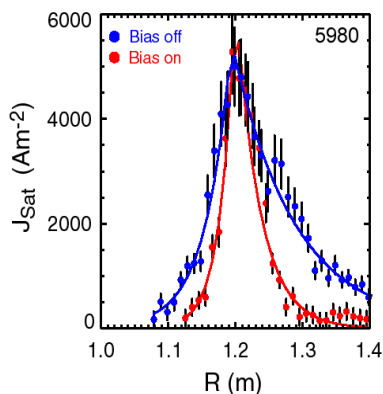


Fig.6 j_{sat}^+ profiles on the un-biased rib with the bias voltage on (red) and off (blue)

6 outer lower divertor ribs were biased for 60ms in the flat top phase of discharge with V_{bias} raised from 0 to 120V over a series of identical Ohmic discharges. The strike points on the biased ribs moved outwards by ~ 3 cm, as monitored by the peak D_α emission, whereas they moved inwards on the un-biased ribs. D_α broadening on the biased ribs and narrowing on the un-biased ribs was observed with no significant changes to the other 3 strike points or core plasma, indicating a localised effect of the divertor biasing, consistent with theory. The j_{sat}^+ profile narrows on the un-biased rib by a factor of 2~3 (see Fig.6) and the total current and power to the un-biased rib falls by $> 25\%$ in spite of the rise in D_α intensity [6].

7. Summary and discussions

Significant progress has been achieved in both SOL and divertor studies, in theory and experiment, during the 3rd physics campaign on MAST, commenced in early 2002. SOL width scaling in the sheath-limited regime revealed weak inverse dependencies on P_{SOL} and q_{95} and stronger positive dependencies on \bar{n}_e and B_T , which is a favourable result for the extrapolation to future machines. The compact size of the ST geometry is offset by the beneficial effects of a large out/in power distribution ratio, including during ELMs. The magnetically symmetric discharge (CDN) is an important requirement for the effective power exhaust. MAST has proved itself suitable for the power amelioration techniques explored in conventional tokamaks such as divertor detachment. The possibility of benefiting from the biased divertor operation in terms of heat flux mitigation is under investigation.

This work is jointly funded by Euratom and UK Department of Trade and Industry. J-W. Ahn and Y. Yang would like to recognise the support, respectively, of a grant from the British Foreign & Commonwealth Office and a Royal Society Fellowship award.

References

- [1] A.Kirk, *et. al.*, An investigation of the effect of B-field variations on the behaviour of the SOL using an advanced Onion-skin Solver, to be submitted to Plasma Physics and Controlled Fusion
- [2] A.Kirk, *et. al.*, ELM characteristics in MAST, 15th PSI conference, Gifu, Japan
- [3] Y.Yang, *et.al.*, Observations with a mid-plane reciprocating probe in MAST, 15th PSI conference, Gifu, Japan
- [4] A.Tabasso, *et.al.*, Analysis of the progress to detachment in the MAST, 15th PSI conference, Gifu, Japan
- [5] D. Ryutov, *et.al.*, On the possibility of inducing strong plasma convection in the divertor of MAST, Plasma Physics and Controlled Fusion 43, 1399
- [6] G.Counsell, *et.al.*, A review of plasma boundary phenomena in the MAST, 15th PSI conference, Gifu, Japan